Enhanced Electrocaloric Response of Vinylidene Fluoride–Based Polymers via One-Step Molecular Engineering

*Florian Le Goupil, Konstantinos Kallitsis, Sylvie Tencé-Girault, Naser Pouriamanesh, Cyril Brochon, Eric Cloutet, Thibaut Soulestin, Fabrice Domingue Dos Santos, Natalie Stingelin, and Georges Hadziioannou**

Electrocaloric refrigeration is one of the most promising environmentally-friendly technologies to replace current cooling platforms—if a notable electrocaloric effect (ECE) is realized around room temperature where the highest need is. Here, a straight-forward, one-pot chemical modification of P(VDF-ter-TrFE-ter-CTFE) is reported through the controlled introduction of small fractions of double bonds within the backbone that, very uniquely, decreases the lamellar crystalline thickness while, simultaneously, enlarging the crystalline coherence along the a-b plane. This increases the polarizability and polarization without affecting the degree of crystallinity or amending the crystal unit cell—undesirable effects observed with other approaches. Specifically, the permittivity increases by >35%, from 52 to 71 at 1 kHz, and ECE improves by >60% at moderate electric fields. At 40 °C, an adiabatic temperature change >2 K is realized at 60 MV m^{-1} (>5.5 K at 192 MV m^{-1}), compared to ≈1.3 K for pristine P(VDF-ter-TrFE-ter-CTFE), highlighting the promise of a simple, versatile approach that allows direct film deposition without requiring any post-treatment such as mechanical stretching or high-temperature annealing for achieving the desired performance.

1. Introduction

The contribution of refrigeration technologies to Greenhouse gases emissions is projected to reach up to 45% by 2050.[1] Moreover, in some western countries, refrigeration consumes up to 25% of the electricity, often produced from non-sustainable sources.[1] The urgency for actions has forced world leaders to agree on global emission targets; among other things, this has driven efforts towards the development of energy-efficient cooling alternatives based on, for example, solid-state cooling.

One particularly promising candidate for solid-state cooling is electrocaloric refrigeration. The electrocaloric effect (ECE) refers to the adiabatic temperature change of a polarizable material under an applied external electric field. An applied field induces a modification of the dipolar states in the material, which results in an entropy decrease ($-\Delta S_{EC}$). In turn, an increase of the material's temperature, ΔT_{EC}, is induced when kept in adiabatic conditions.[2–5] This is reversible. The temperature decreases when the field is removed. This phenomenon can be used to establish a cooling cycle, as schematically illustrated in **Figure 1**a. This cycle is in concept very similar to the one used in conventional vapor-compression refrigeration technology, however, adiabatic polarization/depolarization of a polar solid is used in electrocaloric cooling instead of a compression/decompression of a liquid/gas.

The performance of ECE coolers is directly related to both the adiabatic temperature change ΔT_{EC} of the active material, and its change in entropy, ΔS_{EC}. They both are maximized near structural phase transitions; in ferroelectrics, the Curie temperature (T_c).[2] In order to achieve room temperature cooling, where one of the highest demands in cooling resides,[6,7] materials are required that display a T_c and, hence, a maximum

Dr. F. Le Goupil, Dr. K. Kallitsis, N. Pouriamanesh, Dr. C. Brochon, Dr. E. Cloutet, Prof. N. Stingelin, Prof. G. Hadziioannou
Laboratoire de Chimie des Polymères Organiques (LCPO UMR 5629)
CNRS-Université de Bordeaux-Bordeaux INP
16 Avenue Pey-Berland, Pessac Cedex 33607, France
E-mail: georges.hadziioannou@u-bordeaux.fr

Dr. S. Tencé-Girault
Laboratoire PIMM
Arts et Metiers Institute of Technology
CNRS
Cnam
HESAM University
151 Bd de l'Hopital, Paris 75013, France

Dr. S. Tencé-Girault
Arkema
CERDATO
Route du Rilsan, Serquigny 27470, France

Dr. T. Soulestin, Dr. F. Domingue Dos Santos
Arkema-Piezotech
Rue Henri-Moissan, Pierre-Benite Cedex 69493, France

Prof. N. Stingelin
School of Materials Science and Engineering
Georgia Institute of Technology
771 Ferst Drive, Atlanta, GA 30332, USA

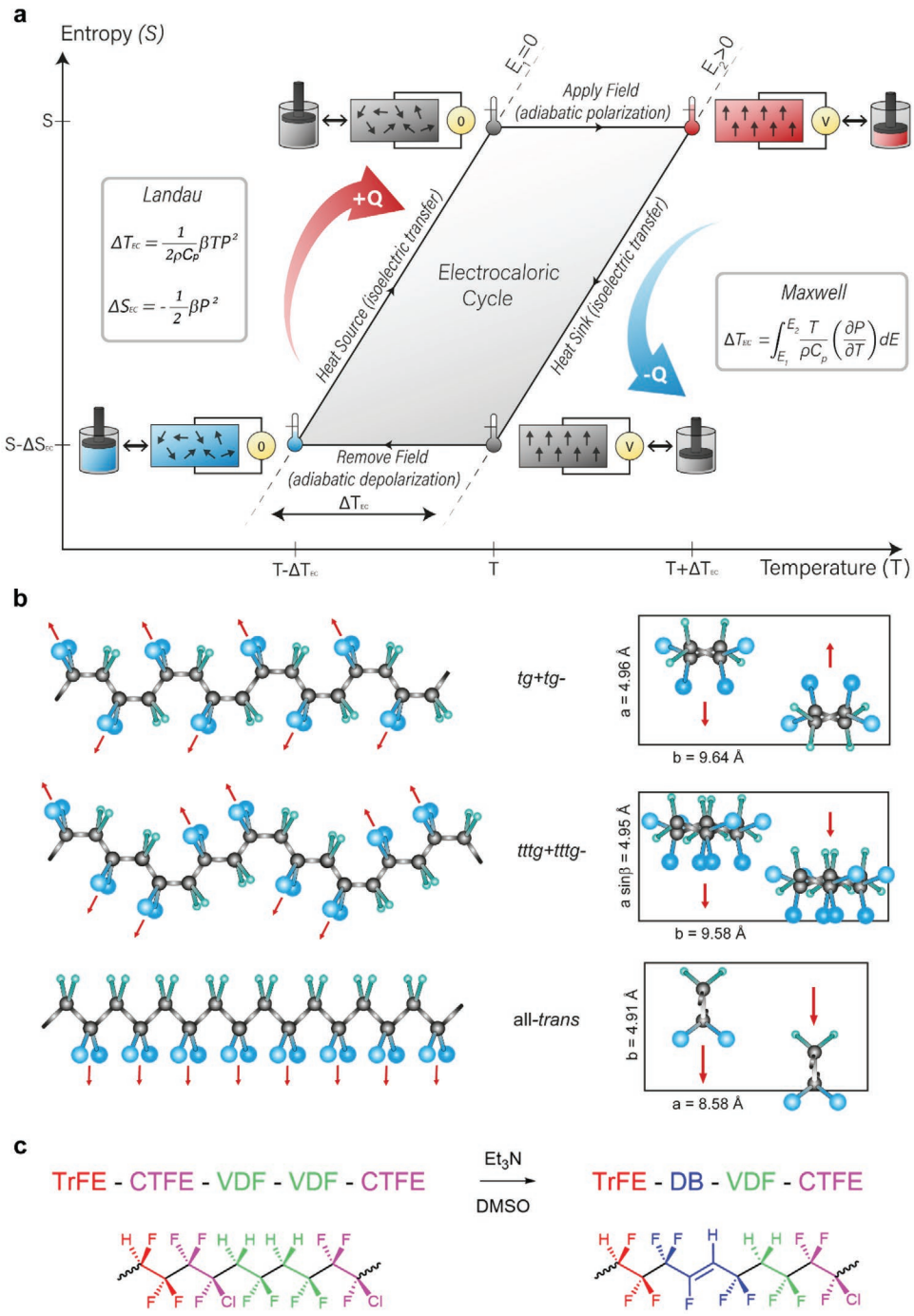

Figure 1. a) Schematic representation of a cooling cycle exploiting the electrocaloric effect. A comparison with a conventional vapor-compression cooling cycle (pistons) is also provided, as well as phenomenological expressions for the electrocaloric entropy, ΔS_{EC}, and the electrocaloric temperature change, ΔT_{EC}. b) Possible chain conformations, that is, tg+tg-, tttg+tttg-, and all-trans[18,19] and corresponding unit cell parameters for poly(vinylidene difluoride) (PVDF). c) Possible monomer units sequence near a de-hydrochlorination site of P(VDF-ter-TrFE-ter-CTFE) upon treatment with triethylamine leading to a small fraction of double bonds (DB).

ECE performance, around room temperature. Electroactive polymers,[8–15] such as poly(vinylidenefluoride-ter-trifluoroethylene-ter-chlorofluoroethylene) P(VDF-ter-TrFE-ter-CFE) and poly(vinylidenefluoride-ter-trifluoroethylene-ter-chlorotrifluoroethylene) P(VDF-ter-TrFE-ter-CTFE), feature transition temperatures near room temperature.[8,16,17] They, thus, have attracted increasing interest over the last ten years.

P(VDF-ter-TrFE-ter-CFE) and P(VDF-ter-TrFE-ter-CTFE) are ter-polymers derived from the common homo-polymer poly(vinylidene fluoride), PVDF. PVDF is known to exhibit several polymorphs depending whether a *tg+tg-* (α-phase), all-*trans* (β-phase), or *tttg+tttg-* (γ-phase) chain conformation is adopted, where *t* stands for *trans* and *g* for *gauche*[18,19] (Figure 1b). The non-polar α-phase is thermodynamically stable at room

temperature, but several approaches exist to stabilize the more sought-after β-phase, which displays a high net dipole moment. Among these approaches, copolymerization of vinylidene fluoride with trifluoroethylene is a commonly used pathway that leads to the random copolymer poly(vinylidene fluoride-*co*-trifluoroethylene) P(VDF-*co*-TrFE). These materials readily crystallize in a ferroelectric phase with a T_c between ≈50 °C and the material's melting temperature, T_m. The precise position of the transition can be manipulated because relevant transition temperatures, including T_m, depend on the TrFE content of the polymer.[20]

The introduction of a bulkier third *co*-monomer, such as chlorofluoroethylene (CFE) or chlorotrifluoroethylene (CTFE), is an additional tool to manipulate T_c. Importantly, this enables to shift this transition temperature (where the ECE is the highest), closer to room temperature,[21] by increasing the crystal cell parameters. It also induces a more diffuse, relaxor-like phase transition, broadening the temperature regime over which high ECEs are observed. This beneficial effect has been attributed to the breaking up of the long-range ferroelectric domains into polar, short-range-ordered nanodomains.[18,21–23] However, while the relaxor properties are desirable to establish an efficient cooling cycle over a broad temperature range, the diffuse nature of the depolarization process in such ter-polymers generally also leads to a lower ECE. Therefore, most of the reported ECE performances at low- to mid-scale electric fields (<100 MV m^{-1}) have so far remained too low for commercial applications (<5 K).

In this paper, we demonstrate a very simple strategy for ECE enhancement in VDF-based ter-polymers through the introduction of a small fraction of double bonds (DB) in their backbones, achieved via a simple de-hydrochlorination step of P(VDF-ter-TrFE-ter-CTFE) that leads to an increase of the polarization at low field and an increase in their polarizability. De-hydrochlorination of fluorinated polymers has been used before, to enable crosslinking and facilitate uniaxial stretching, however, relatively high amounts of double-bond defects were generally introduced often leading to a drastic reduction in crystallinity.[24–27] In contrast, we introduced double bonds into the polymer backbones (up to 5.8%) to extend the coherence of the molecular order along the *a*–*b* planes of the material's crystalline moieties (i.e., along the polar direction)[28,29] via, for example, favorable π–π interactions between macromolecular segments that can nucleate ordering and packing. This should increase the net dipole of the crystalline regions. The introduction of DBs also should stabilize the more polar conformations in the material. As a consequence of both these changes, the maximum polarization P should increase. Considering that $\Delta S_{EC} = -\frac{1}{2}\beta P^2$ for $T > T_c$, where β is a materials specific constant,[30,31] ΔS_{EC} is thus expected to be enhanced and, in turn, ΔT_{EC}.

A high ΔS_{EC} is, however, not sufficient to produce an energy-efficient cooling cycle, as already alluded to above. A high ΔS_{EC} is only useful if it can be achieved at sufficiently low electric fields. Therefore, a high change in polarization with field (dP/dE)—that is, a high polarizability—needs to be realized in materials used for electrocaloric cooling. Since the introduction of double bonds introduces "defects" along the polymer backbone (in addition to those produced via co-polymerization), it may further decrease parameters such as the lamellar crystal thickness.[32] This has been reported to lower the energy barrier for dipole flipping to occur (see, e.g., ref. [15]), thus, increasing the material's polarizability.

2. Results and Discussion

In order to produce P(VDF-ter-TrFE-ter-CTFE) polymers with a controlled, minute fraction of double bonds, the materials were treated with a weak base, namely triethylamine, following the reaction shown in Figure 1c. A de-hydrochlorination occurs through a nucleophilic attack of triethylamine on a VDF-CTFE sequence, leading to the formation of DBs as detailed in Scheme S1 (Supporting Information). Changing the base equivalent, reaction time and temperature of this simple modification allowed a good control of the DB content (Table S1, Supporting Information), as evidenced by the ^{1}H NMR of the DB-modified ter-polymers.

We selected five different DB-modified P(VDF-ter-TrFE-ter-CTFE) with DB contents ranging from 0.6% to 5.8% (evaluated from the ^{1}H NMR data, using the equation given in Figure S1, Supporting Information) in order to have a comprehensive series to elucidate how the introduction of DBs affects the ECE.

Promisingly, a gradual increase of the maximum of permittivity at 1 kHz, ε_{max}, is observed with increasing DB content, reaching a maximum value of $\varepsilon_{max} \approx 71$ for the material with 5% DB content, compared with $\varepsilon_{max} \approx 52$ for the pristine polymer (**Figure 2**a). This corresponds to an increase in permittivity of more than 35%. Note, however, that when the DB-content was increased to 5.8%, the maximum permittivity started to decrease. We attribute this behavior to an increased dielectric loss at higher DB content (see Figure 2a, inset), likely because of the creation of conjugated, or partially conjugated, chain segments. We observe indeed that materials comprising 5.8% DB have a yellowish appearance typical for species featuring short, conjugated segments. In addition, a weak, broad vibrational feature between 1525 and 1650 cm^{-1} is recorded via Raman spectroscopy, characteristic for conjugated double bonds (isolated DB display vibrations a 1720 cm^{-1}; Figure S2, Supporting Information). This highlights the need for a high control of the double bond content introduced by the modification. By tuning the reaction conditions to be sufficiently mild, only small amounts of double bonds are introduced, leading to dielectric properties superior to the highest reported values for de-hydrochlorinated materials of high DB content,[27] while eliminating the need for additional processing steps, such as high-temperature crosslinking or uniaxial stretching. The need for extra processing steps drastically reduces, among other things, the manufacturing flexibility with respect to the type of architectures the materials can be applied in.

Further evidence of the increased polarizability that can be achieved by the introduction of a rather minute amounts of double bonds can be inferred from the lowering of the electric field, E_C, needed to induce maximum cooperative forces between dipoles. In DB-modified ter-polymers, we identified E_C from the peak currents indicated in Figure 2c with dotted lines. Since the highest permittivity was measured for 5% DB, we focused on ter-polymers with this specific DB content and compared their behavior with pristine P(VDF-ter-TrFE-ter-CTFE). A notable decrease of E_c from 47 MV m^{-1} for the pristine polymer, to 35 MV m^{-1} for the modified materials (5% DB) is observed, illustrating the significant and positive effect that the

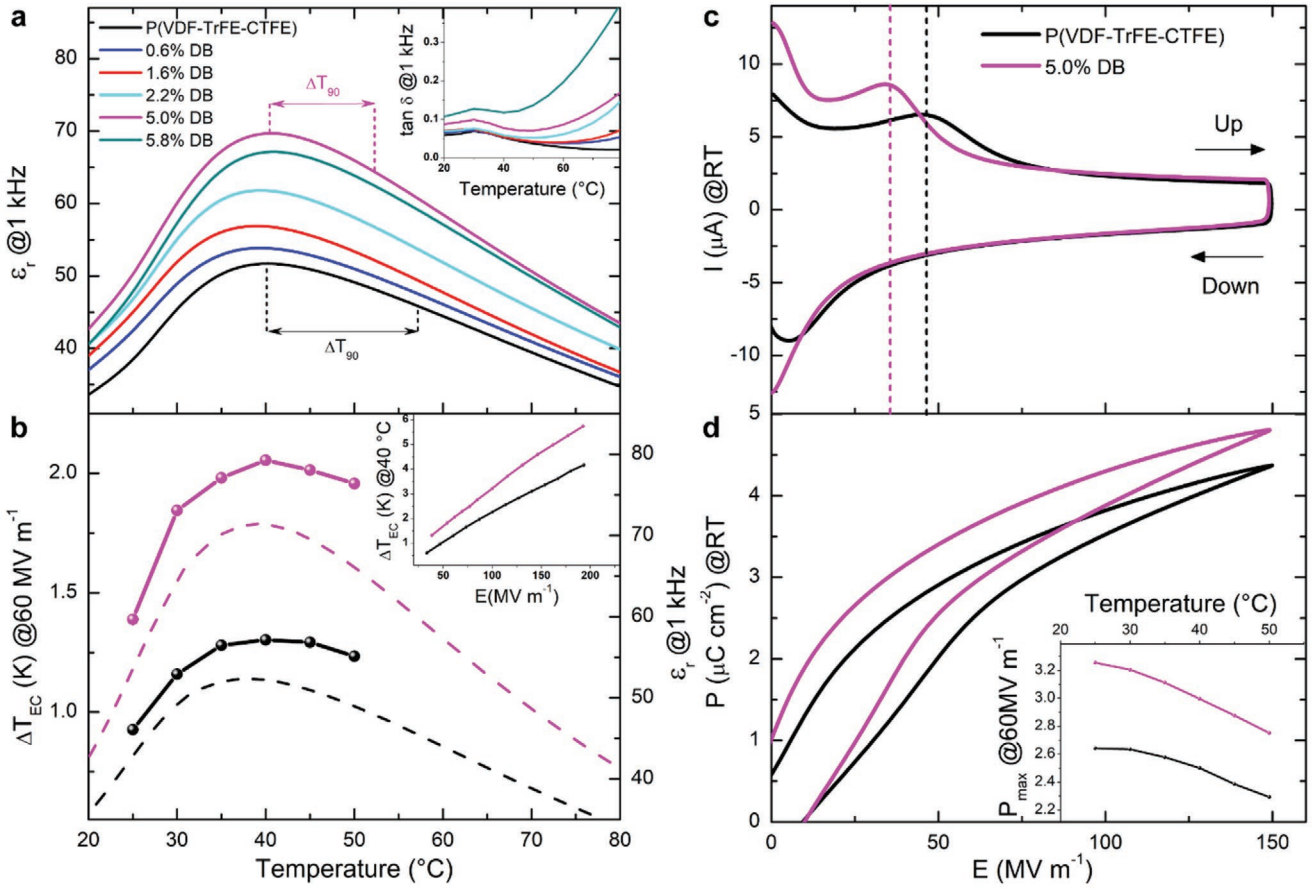

Figure 2. a) Real part of the permittivity versus temperature measured on the pristine ter-polymer and modified P(VDF-ter-TrFE-ter-CTFE) materials of different DB content. The inset shows the temperature dependence of the dielectric loss. b) Electrocaloric adiabatic temperature change versus temperature at 60 MV m^{-1} obtained for both the pristine P(VDF-ter-TrFE-ter-CTFE) and its 5%-DB-modified counterpart from direct calorimetry measurements. The corresponding real part of the permittivity measured at 1 kHz is also given (dotted lines). The inset shows the electrocaloric adiabatic temperature change versus applied electric field measured at 40 °C, using fields of up to 192 MV m^{-1}. c) Current versus electric field measured at RT and 10 Hz for both the pristine P(VDF-ter-TrFE-ter-CTFE) and its 5%-DB-modified counterpart. d) Polarization versus electric field (P–E loop) for both the pristine P(VDF-ter-TrFE-ter-CTFE) and its 5%-DB-modified counterpart measured at 10 Hz, with a maximum field of 150 MV m^{-1}. The inset shows the temperature evolution of the maximum polarization measured at 60 MV m^{-1}.

introduction of this rather small fraction of DB can have on the materials properties.

Beneficially, not only the polarizability of the modified polymers increased, we also found a higher polarization, *P*, in materials comprising DBs. This can be deduced from the polarization versus electric field dependencies, commonly referred to as P-E loop, shown in Figure 2d for materials with 5% DB and the pristine polymer, measured at room temperature. The polarization, *P*, at a moderate electric field of 60 MV m^{-1}, increases from 2.6 μC cm^{-2} for the pristine polymer, to 3.2 μC cm^{-2} for the material comprising 5% DB. Furthermore, the polarization of the DB-modified polymer is enhanced over the entire temperature range studied (Figure 2d, inset).

This significant increase in polarization combined with the increase in polarizability leads to a significant ECE enhancement in DB-modified materials. Figure 2b shows, for instance, the adiabatic temperature change, ΔT_{EC}, that we recorded at 60 MV m^{-1} for both the pristine P(VDF-ter-TrFE-ter-CTFE) and its 5%-DB-modified counterpart over a broad temperature range using an in-house modified differential scanning calorimeter (DSC) that allows a direct measurement of ΔT_{EC}.[5] At a moderate field of 60 MV m^{-1}, the maximum adiabatic temperature change ΔT_{EC} for the DB-modified polymer is 2.1 K. At the same electric field and temperature, the pristine P(VDF-ter-TrFE-ter-CTFE) displays a ΔT_{EC} of only 1.3 K. This corresponds to an ECE enhancement of more than 60%. (NB: The corresponding real part of the dielectric permittivity versus temperature measured at 1 kHz is given with dotted lines to indicate the transition temperature). The ECE enhancement is maintained over the whole range of electric fields studied, leading at 40 °C to a ΔT_{EC} of 5.7 K at a field of 192 MV m^{-1} (Figure 2b, inset).

Most reassuringly, the observed ECE enhancements between pristine and modified polymers agree well with predictions based on the Landau phenomenological approach (Figure 1; see for more details Notes S1, Supporting Information), preferred to the more controversial Maxwell approach,[9] employing experimentally obtained data extracted from Figure 2d; that is, a maximum polarization, P_{max}, at 60 MV m^{-1} of 2.5 μC cm^{-2} for the pristine polymer and 3 μC cm^{-2} for the modified polymer with 5% DB. Using ρ = 1800 kg m^{-3} and c_p = 1400 J kg^{-1} K^{-1} from literature,[33,34] an increase of ECE from ΔT_{EC} of 1.5 K for the pristine polymer to ΔT_{EC} of 2.2 K for modified materials comprising 5% DB at 60 MV m^{-1} is calculated, in close agreement with our experimentally established values, supporting the validity of our direct DSC measurements.

The ECE enhancement is also in good agreement with the observed decrease of the width of the permittivity peak, given by the difference between the temperature of maximum permittivity and the temperature at which the permittivity is decreased by 10% upon heating,[35] commonly referred to as ΔT_{90} and indicated in Figure 2a. ΔT_{90} decreases in DB-modified materials: from 17 K for the untreated material to 13 K for the modified polymer (5% DB), both measured at 1 kHz. According to the Maxwell-equation-derived expression of the ECE given in Figure 1a, ΔT_{EC} varies with $(dP/dT)_E$. With $P = \varepsilon_0 \cdot \varepsilon_r \cdot E$ and, thus, $(dP/dT)_E = \varepsilon_o \cdot E\ (d\varepsilon_r/dT)_E$, a sharper phase transition should result in a higher ECE, as we observe.

The notable enhancement of the ECE effect found in the treated polymers comprising a small fraction of DBs in their backbones can be directly correlated with changes in important structural features crossing multiple lengths scales. Thereby, commonly used parameters such as "crystallinity" and/or "crystal size" are not sufficient to establish clear structural dependencies.[15,36,37]

The observed enhancement in the materials' polarizability, illustrated by the increased permittivity and the decreased E_c, results from a unique combination, not achieved so far with other approaches,[15,36,37] of crystal thinning along the polymer backbone direction, and an increase in the coherence of the lateral crystalline order (i.e., the coherence within the *a*–*b* planes of the crystalline moieties), without decreasing the overall degree of crystallinity. The crystal thinning lowers the energy barrier for dipole flipping because the coherence length along the chain directions is shortened. The extended correlation length of the crystalline lamellae in the lateral directions increases the number of dipoles that can be oriented in the polar direction, also contributing to easier dipole flipping; it also is beneficial for achieving a high polarization, especially as the degree of crystallinity is not affected by our modification.

Evidence for crystal thinning in the chain direction is obtained from the small-angle X-ray scattering (SAXS) data presented in **Figure 3**a, showing a correlation peak characterizing the period organization of the crystalline lamellae. The

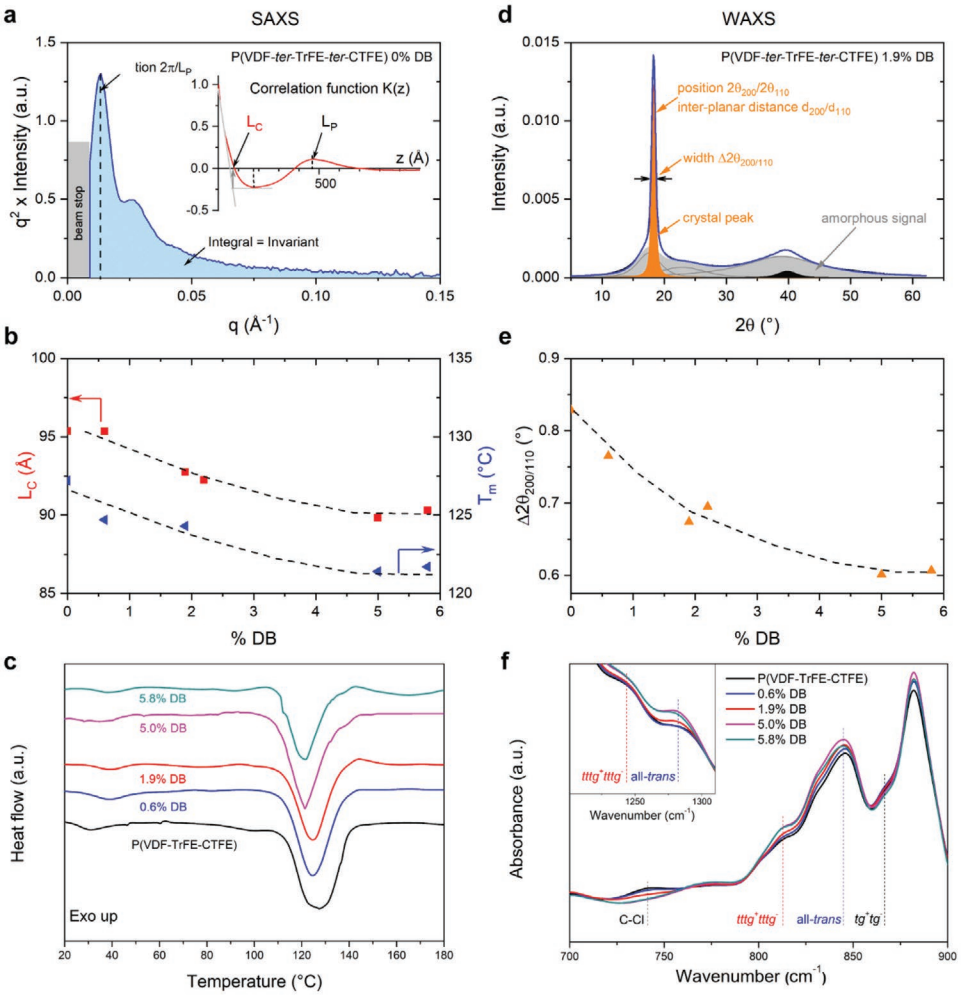

Figure 3. a) Lorentz-corrected SAXS spectra, $q^2 \cdot I(q)$, measured for the pristine P(VDF-ter-TrFE-ter-CTFE) polymer. Its correlation function K(z) is shown in the inset. b) Evolution as function of DB content of the crystalline lamellae thickness, L_C, extracted from SAXS, and melting temperature, T_m, extracted from differential scanning calorimetry (DSC). c) DSC thermograms (first heating) measured for the pristine ter-polymer and modified P(VDF-ter-TrFE-ter-CTFE) materials of different DB content, using a heating rate of at 10 °C min^{-1}. d) WAXS spectra measured on a modified P(VDF-ter-TrFE-ter-CTFE) polymer with a 1.9% DB content, where the crystalline (orange) and amorphous (grey) contributions are decomposed as indicated. e) Width-at-half-maximum, $\Delta 2\theta_{200/110}$, of the Bragg peak versus DB content. f) ATR FT-IR spectra measured at RT on the pristine and modified P(VDF-ter-TrFE-ter-CTFE) polymers of different DB content.

correlation function K(z) calculated from this SAXS spectrum is shown in the inset. We used K(z) to deduce the thickness of the crystalline lamellae, L_C (illustrated schematically in **Figure 4**a), from the intersection between the two tangents shown in the inset of Figure 3a (see for more details Notes S2, Supporting Information). We find that L_C gradually decreases with increasing DB content, from 95 Å for the pristine polymer, to 90 Å for materials comprising 5% and 5.8% DB (**Table 1**). This is in agreement with the gradual change in melting temperature that we observe in differential scanning calorimetry (DSC), from ≈127 °C down to 121 °C (Figure 3b,c). [NB: T_m is directly correlated to L_C via the Gibbs-Thomson equation.[38,39]] The long period, L_P, which provides information on the periodic arrangement of the crystalline lamellae and amorphous regions (Figure 4a), in contrast, is essentially unaffected by the DB modification (Figure S5d, Supporting Information).

Wide-angle X-ray scattering (WAXS) provided us with insights on the lateral coherence of the crystalline moieties in pristine and DB-modified polymers (Figure 3d). We thereby focused on the Bragg peak resulting from the juxtaposition

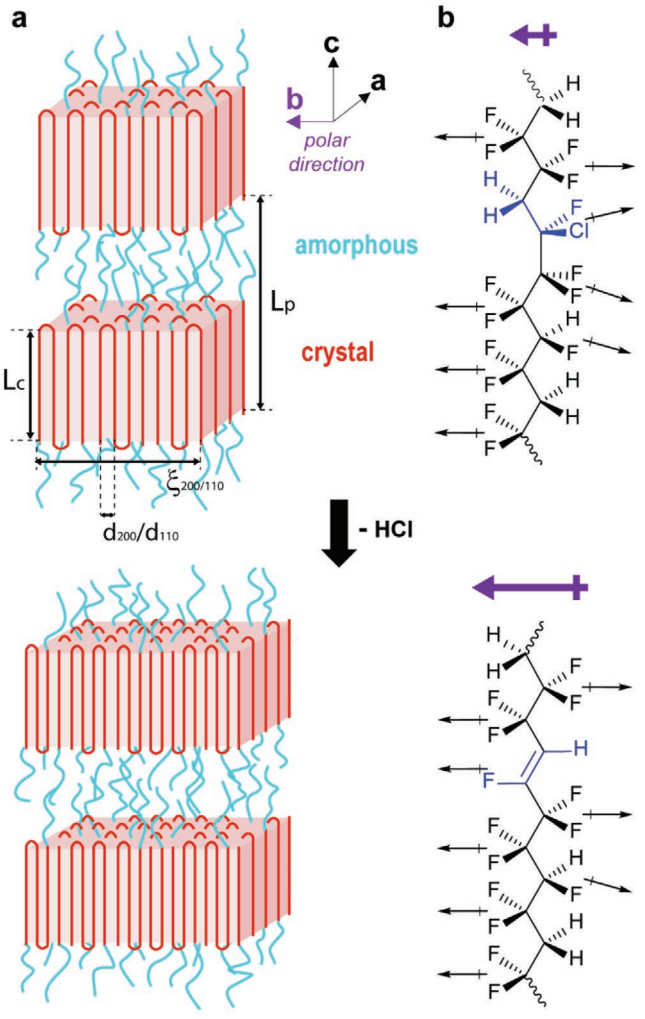

Figure 4. Schematic illustration of the evolution of a) the crystalline lamellae and b) the chain conformation when introducing double-bond defects in the backbone of P(VDF-ter-TrFE-ter-CTFE). The site of the dehydrochlorination is highlighted in blue; the net dipole is given in purple.

of the two diffraction lines resulting from the (200) and (110) planes, (shaded in orange in Figure 3d), which can be associated with the inter-planar distance, d_{200}/d_{110}, of the orthorhombic pseudo-hexagonal phase, often referred to as RFE (Relaxor FerroElectric) structure, as described in a previous work.[21]

Some observations can be made: the width-at-half maximum, $\Delta 2\theta_{200/110}$, of this Bragg peak gradually decreases from 0.83° to ≈0.60° when going from the pristine polymer to the modified materials with 5% and 5.8% DB (Figure 3e). In contrast, the inter-planar distance d_{200}/d_{110} is essentially unaffected by the introduction of low DB contents (≤3%) with d_{200}/d_{110} ≈ 4.84 Å for all low-DB-content materials; however, d_{200}/d_{110} abruptly decreases to ≈4.81 Å in polymers comprising higher DB contents (5% and 5.8%; see Table 1). Since the $\Delta 2\theta_{200/110}$, is more correlated with the DB fraction than the inter-planar distance d_{200}/d_{110} (Figure S5, Supporting Information), we conclude that the decrease in $\Delta 2\theta_{200/110}$ is not because of an evolution of the cell parameters but, rather, resulting from a lateral extension of the crystalline moieties in the material (i.e., an extension of the coherence length of the crystalline order perpendicular to the polymer backbone, $\xi_{200/110}$, indicated in Figure 4a), likely because of the favorable influence of π–π interactions that nucleate order perpendicular to the backbone direction. If $\Delta 2\theta_{200/110}$ were reduced because of cell parameters evolution, as found, for instance, during a phase transition, a clear correlation between $\Delta 2\theta_{200/110}$ and d_{200}/d_{110} would be observed.[40]

Similar to the polarizability, the high maximum polarization that can be achieved with DB-modified polymers seems to have two structural origins as well. On the molecular level, the ratio of polar/apolar conformations, as inferred from Fourier-transform infrared (FT-IR) spectroscopy (bands at 811, 845, 1244, and 1283 cm^{-1} for polar all-*trans* and *tttg+tttg*-conformations, and 867 cm^{-1} for the apolar *tg+tg*-conformation) increases systematically with increasing DB content (Figure 3f). The reason is that with increasing DB content, introduced via the de-hydrochlorination reaction, the amount of CTFE moieties, which often lead to apolar gauche conformations in their vicinity, is decreased. We can follow this reduction of CTFE content by tracing the 741 cm^{-1} band in FT-IR spectroscopy, which is characteristic for the presence of C—Cl bonds. Since most probably the reaction proceeds via an E2 pathway (Scheme S1, Supporting Information), exclusively double bonds in the *trans* configuration are formed, further stabilizing all-*trans* and *tttg+tttg*-conformations of P(VDF-ter-TrFE-ter-CTFE), thus, enhancing the net dipole moment of the materials and, in turn, further increasing the maximum polarization that can be obtained with DB-modified polymers. The replacement of $-CClF-CH_2-$ (CFE) with a fluorine bearing DB unit, that is, with $-CF=CH-$, which has a dipole moment that is even higher than that of the VDF-moiety (>2.1 D) due to the alignment in the polar direction of the C—F and C—H bonds around the DB, thereby, additionally contributes to the already increased net dipole moment (the dipole moment of CFE is 1.8 D[41]). This enhancement in net dipole moment in materials after de-hydrochlorination is highlighted in Figure 4b in purple; the site responsible for the conformation change (—CFE) is given in blue.

On a larger length scale, the polarization in DB-modified polymers is increased through densification of the crystalline phase, leading to a higher dipole moment per volume in these

Table 1. Parameters extracted from the SAXS and WAXS analysis for the pristine polymer and a set of materials with different double-bond content. Given are: the inter-planar distances, d_{200}/d_{110}, the width-at-half maxima of the Bragg peak, $\Delta 2\theta_{200/110}$, and the degree of crystallinity, χ_c, as deduced from WAXS; and the long periods, L_P, the thicknesses of the crystalline lamellae, L_C, as well as the invariants, obtained from SAXS.

	d_{200}/d_{110} [Å]	$\Delta 2\theta_{200/110}$ [°]	χ_C	L_P [Å]	L_C [Å]	Invariant [a.u.]
P(VDF-ter-TrFE-ter-CTFE)	4.84	0.83	0.24	474	95	0.37
0.6% DB	4.84	0.77	0.22	484	95	0.39
1.9% DB	4.85	0.67	0.22	492	93	0.40
2.2% DB	4.84	0.70	0.24	473	92	0.37
5.0% DB	4.82	0.60	0.24	462	90	0.45
5.8% DB	4.81	0.61	0.26	475	90	0.48

regions. We infer the increase in crystalline density from the integration of the Lorentz-corrected SAXS spectra, $q^2 \cdot I$ (q), of the pristine polymer and the DB-modified materials, which gives us the invariant of these systems (Table 1, and Figure S5b, Supporting Information). The invariant, which increases significantly for higher DB contents, depends on the contrast given by the square of the density difference between crystalline and amorphous phases $(\rho_c - \rho_a)^2$. An increase of the invariant is a clear indication of a densification of the crystalline phase and, thus, the crystalline quality, in DB-modified polymers of a DB content of 5% and 5.8%. This view is supported by the fact that we also observed a decrease in interplanar distance d_{200}/d_{110} at a DB content ≥5% (Figure S5c, Supporting Information).

Finally, we would like to stress that the chemical modification does not negatively affect the overall degree of crystallinity, χ_c, of DB-modified ter-polymers compared to the pristine material, in contrast to previous approaches introducing larger fractions of double bonds enabling crosslinking and mechanical stretching.[24–27] We qualitatively deduced this from the differential scanning calorimetry thermograms displayed in Figure 3c, where we record very similar enthalpies of fusion, ΔH_m, for the different materials, with ΔH_m generally being directly linked with χ_c. More quantitatively, χ_c were extracted from the WAXS data in Figure S4 (Supporting Information) as shown in Figure S5a (Supporting Information). For all materials, we find that the materials comprise 24% ± 2% crystalline fractions (**Table 1**), independent on the DB content. This is in contrast to many approaches where modification of VDF-based materials leads to a reduction of the degree of crystallinity. One of the few exceptions, where the degree of crystallinity seems to be increased, exploits polymer confinement in nanoporous aluminum oxide.[15] While very elegant for fundamental studies, this method requires tedious sample manipulation—in stark contrast to our simple chemical modification that can be achieved, on large scale, via a one-pot synthesis procedure.

3. Conclusion

In summary, we have used a straight-forward chemical modification that allows to produce P(VDF-ter-TrFE-ter-CTFE) derivatives of a high polarization and high polarizability, and thus, enhanced ECE, without incorporation of further bulky substituents (which often detrimentally affect the overall degree of crystallinity/molecular packing within the crystalline domains), or use of complex processing methodologies, such as confinement in nano-porous oxides. Indeed, our approach of incorporating a sufficiently small fraction of double bonds in the material's backbones allows us to introduce a desirable amount of polar configurations that lead to an increase in both the local dipole and the general maximum polarization that can be achieved. The polarizability is also enhanced because of a decrease in the crystalline dimensions along the polymer backbone direction, lowering the energy barrier for dipole flipping, while the crystal dimensions parallel to the polarization direction are extended at the same time. The degree of crystallinity stays thereby essentially unchanged; however, the density of crystalline regions increases, indicating an improvement in the crystalline quality—in strong contrast to previous de-hydrochlorination approaches where relatively large numbers of double bonds were introduced to enable mechanical stretching and crosslinking, generally lowering the overall crystallinity.[24–27] Further progress seems possible, especially if formation of conjugated double bonds units can be prevented. Clear is that our approach is widely applicable, as high-performing structures can be obtained as-cast (i.e., without the need for post-treatment), providing new promise for PVDF derivatives for low-temperature electrocaloric cooling.

Acknowledgements

F.L.G. and K.K. contributed equally to this work. The research leading to these results has received funding from the People Programme (Marie Curie Actions) of the European Union's Seventh Framework Programme (FP7/2007-2013) under REA grant agreement n. PCOFUND-GA-2013-609102, through the PRESTIGE programme coordinated by Campus France. The authors also acknowledge the financial support from Arkema and Région Nouvelle Aquitaine as well as from the Industrial Chair HOMERIC (Arkema/ANR) within the grant agreement no. AC-2013-365. K.K. acknowledges the Région Nouvelle Aquitaine for the financial support (Ph.D. grant #2015-1R10207-00004862). This work was performed within the framework of the Equipex ELORPrintTec ANR-10-EQPX-28-01 with the help of the French state's Initiative d'Excellence IdEx ANR-10-IDEX-003-02. S.T.-G's contribution was achieved within the framework of the Industrial Chair

Arkema (Arkema/CNRS-ENSAM-Cnam). N.S. acknowledges the IDEx Associated International Chair entitled MARBLE.

Conflict of Interest

The authors declare no conflict of interest.

Keywords

electrocaloric effect, ferroelectric polymer, microstructure tuning

[1] J. Shi, D. Han, Z. Li, L. Yang, S.-G. Lu, Z. Zhong, J. Chen, Q. M. Zhang, X. Qian, *Joule* **2019**, *3*, 1200.
[2] T. Correia, Q. Zhang, *Electrocaloric Materials*, Springer, Berlin **2014**.
[3] X. Moya, S. Kar-Narayan, N. D. Mathur, *Nat. Mater.* **2014**, *13*, 439.
[4] V. Matjaz, *Prog. Mater. Sci.* **2012**, *57*, 980.
[5] F. L.e Goupil, A. Berenov, A.-K. Axelsson, M. Valant, N. M. Alford, *J. Appl. Phys.* **2012**, *111*, 124109.
[6] X.-S. Qian, H.-J. Ye, Y.-T. Zhang, H. Gu, X. Li, C. A. Randall, Q. M. Zhang, *Adv. Funct. Mater.* **2014**, *24*, 1300.
[7] F. L.e Goupil, R. McKinnon, V. Koval, G. Viola, S. Dunn, A. Berenov, H. Yan, N. M. Alford, *Sci. Rep.* **2016**, *6*, 28251.
[8] B. Neese, B. Chu, S.-G. Lu, Y. Wang, E. Furman, Q. M. Zhang, *Science* **2008**, *321*, 821.
[9] S. G. Lu, B. Rozic, Q. M. Zhang, Z. Kutnjak, R. Pirc, M. R. Lin, X. Y. Li, L. Gorny, *Appl. Phys. Lett.* **2010**, *97*, 202901.
[10] X. Chen, X. Qian, X. Li, S. G. Lu, H. Gu, M. Lin, Q. Shen, Q. M. Zhang, *Appl. Phys. Lett.* **2012**, *100*, 222902.
[11] H. Gu, X. Qian, X. Li, B. Craven, W. Zhu, A. Cheng, S. C. Yao, Q. M. Zhang, *Appl. Phys. Lett.* **2013**, *102*, 122904.
[12] D. Guo, J. Gao, Y.-J. Yu, S. Santhanam, G. K. Fedder, A. J. H. McGaughey, S. C. Yao, *Appl. Phys. Lett.* **2014**, *105*, 031906.
[13] R. Ma, Z. Zhang, K. Tong, D. Huber, R. Kornbluh, Y. S. Ju, Q. Pei, *Science* **2017**, *357*, 1130.
[14] J. Qian, M. Guo, J. Jiang, Z. Dan, Y. Shen, *J. Mater. Chem. C* **2019**, *7*, 3212.
[15] G. Zhang, L. Weng, Z. Hu, Y. Liu, R. Bao, P. Zhao, H. Feng, N. Yang, M.-Y. Li, S. Zhang, S. Jiang, Q. Wang, *Adv. Mater.* **2019**, *31*, 1806642.
[16] G. Sebald, L. Seveyrat, J.-F. Capsal, P.-J. Cottinet, D. Guyomar, *Appl. Phys. Lett.* **2012**, *101*, 022907.
[17] V. Basso, F. Russo, J.-F. Gerard, S. Pruvost, *Appl. Phys. Lett.* **2013**, *103*, 202904.
[18] T. Soulestin, V. Ladmiral, F. D. D. Santos, B. Améduri, *Prog. Polym. Sci.* **2017**, *72*, 16.
[19] A. J. Lovinger, *Science* **1983**, *220*, 1115.
[20] K. Tashiro, M. Kobayashi, *Phase Transitions* **1989**, *18*, 213.
[21] F. Bargain, D. Thuau, P. Panine, G. Hadziioannou, F. D. D. Santos, S. Tencé-Girault, *Polymer* **2019**, *161*, 64.
[22] L. Yang, X. Li, E. Allahyarov, P. L. Taylor, Q. M. Zhang, L. Zhu, *Polymer* **2013**, *54*, 1709.
[23] L. Zhu, *J. Phys. Chem. Lett.* **2014**, *5*, 3677.
[24] S. Tan, J. Li, G. Gao, H. Li, Z. Zhang, *J. Mater. Chem.* **2012**, *22*, 18496.
[25] S. Tan, X. Hu, S. Ding, Z. Zhang, H. Li, L. Yang, *J. Mater. Chem. A* **2013**, *1*, 10353.
[26] Y. Zhang, S. Tan, J. Wang, X. Wang, W. Zhu, *Z. Zhang, Polymers* **2018**, *10*, 339.
[27] Z. Zhang, X. Wang, S. Tan, Q. Wang, *J. Mater. Chem. A* **2019**, *7*, 5201.
[28] K. Kallitsis, D. Thuau, T. Soulestin, C. Brochon, E. Cloutet, F. D. D. Santos, G. Hadziioannou, *Macromolecules* **2019**, *52*, 5769.
[29] K. Kallitsis, T. Soulestin, S. Tencé-Girault, C. Brochon, E. Cloutet, F. D. D. Santos, G. Hadziioannou, *Macromolecules* **2019**, *52*, 8503.
[30] J. G. Webster, Z. Kutnjak, B. Rožič, R. Pirc, *Wiley Encyclopedia of Electrical and Electronics Engineering*, John Wiley and Sons, Inc., **2015**.
[31] J. Gong, A. J. H. McGaughey, *Int. J. Energy Res.* **2020**, *44*, 5343.
[32] T. C. Chung, A. Petchsuk, *Macromolecules* **2002**, *35*, 7678.
[33] P. F. Liu, J. L. Wang, X. J. Meng, J. Yang, B. Dkhil, J. H. Chu, *New J. Phys.* **2010**, *12*, 023035.
[34] S. G. Lu, B. Rozic, Z. Kutnjiak, Q. M. Zhang, *Integr. Ferroelectr.* **2011**, *125*, 176.
[35] F. L.e Goupil, A.-K. Axelsson, M. Valant, T. Lukasiewicz, J. Dec, A. Berenov, N. M. Alford, *Appl. Phys. Lett.* **2014**, *104*, 222911.
[36] X.-Z. Chen, X. Li, X.-S. Qian, S. Wu, S.-G. Lu, H.-M. Gu, M. Lin, Q.-D. Shen, Q. M. Zhang, *Polymer* **2013**, *54*, 2373.
[37] Q. Li, G. Zhang, X. Zhang, S. Jiang, Y. Zeng, Q. Wang, *Adv. Mater.* **2015**, *27*, 2236.
[38] J. W. Gibbs, H. A. Bumstead, R. G. Van Name, W. R. Longley, *The Collected Works of J. Willard Gibbs*, Longmans, Green And Co., New York **1902**.
[39] J. J. Thomson, *Applications of Dynamics to Physics and Chemistry*, Adamant Media Corporation, Boston, MA **2005**.
[40] F. Bargain, P. Panine, F. D. D. Santos, S. Tencé-Girault, *Polymer* **2016**, *105*, 144.
[41] L. Yang, B. A. Tyburski, F. D. D. Santos, M. K. Endoh, T. Koga, D. Huang, Y. Wang, L. Zhu, *Macromolecules* **2014**, *47*, 8119.